

# AU+AU COLLISIONS AT 40-150 MEV/NUCLEON: FROM PERIPHERAL TO CENTRAL

J. Łukasik<sup>6,10</sup>, W. Trautmann<sup>6</sup>, F. Lavaud<sup>2</sup>, E. Plagnol<sup>2</sup>, G. Auger<sup>1</sup>, Ch.O. Bacri<sup>2</sup>, M.L. Begemann-Blaich<sup>6</sup>, N. Bellaïze<sup>3</sup>, R. Bittiger<sup>6</sup>, F. Bocage<sup>3</sup>, B. Borderie<sup>2</sup>, R. Bougault<sup>3</sup>, B. Bouriquet<sup>1</sup>, Ph. Buchet<sup>4</sup>, J.L. Charvet<sup>4</sup>, A. Chbihi<sup>1</sup>, R. Dayras<sup>4</sup>, D. Doré<sup>4</sup>, D. Durand<sup>3</sup>, J.D. Frankland<sup>1</sup>, E. Galichet<sup>5</sup>, D. Gourio<sup>6</sup>, D. Guinet<sup>5</sup>, S. Hudan<sup>1</sup>, B. Hurst<sup>3</sup>, P. Lautesse<sup>5</sup>, J.L. Laville<sup>1</sup>, C. Leduc<sup>5</sup>, A. Le Fèvre<sup>6</sup>, R. Legrain<sup>4</sup>, O. Lopez<sup>3</sup>, U. Lynen<sup>6</sup>, W.F.J. Müller<sup>6</sup>, L. Nalpas<sup>4</sup>, H. Orth<sup>6</sup>, E. Rosato<sup>7</sup>, A. Saija<sup>8</sup>, C. Sfienti<sup>6</sup>, C. Schwarz<sup>6</sup>, J.C. Steckmeyer<sup>3</sup>, G. Tăbăcaru<sup>1</sup>, B. Tamain<sup>3</sup>, A. Trzciński<sup>9</sup>, K. Turzó<sup>6</sup>, E. Vient<sup>3</sup>, M. Vigilante<sup>7</sup>, C. Volant<sup>4</sup>, B. Zwiegliński<sup>9</sup> and A.S. Botvina<sup>6</sup> (The INDRA and ALADIN Collaborations)

<sup>1</sup> GANIL, CEA et IN2P3-CNRS, B.P. 5027, F-14076 Caen, France

<sup>2</sup> Institut de Physique Nucléaire, IN2P3-CNRS et Université, F-91406 Orsay, France

<sup>3</sup> LPC, IN2P3-CNRS, ISMRA et Université, F-14050 Caen, France

<sup>4</sup> DAPNIA/SPhN, CEA/Saclay, F-91191 Gif sur Yvette, France

<sup>5</sup> Institut de Physique Nucléaire, IN2P3-CNRS et Université F-69622 Villeurbanne, France

<sup>6</sup> Gesellschaft für Schwerionenforschung mbH, D-64291 Darmstadt, Germany

<sup>7</sup> Dipartimento di Scienze Fisiche e Sezione INFN, Univ. Federico II, I-80126 Napoli, Italy

<sup>8</sup> Dipartimento di Fisica dell' Università and INFN I-95129 Catania, Italy

<sup>9</sup> A. Sołtan Institute for Nuclear Studies, PL-00681 Warsaw, Poland

<sup>10</sup> H. Niewodniczański Institute of Nuclear Physics, PL-31342 Kraków, Poland

## Abstract

Experimental data obtained with the use of the  $4\pi$  multi-detector system INDRA and the beams delivered by the SIS synchrotron facility at GSI, were used to study peripheral and central collisions of Au and Au at energies between 40 and 150 MeV/nucleon. The analysis was performed as a function of incident energy and of centrality of the collision, defined through the total transverse energy (E<sub>trans12</sub>) of light charged particles (LCP,  $Z \leq 2$ ). Transverse velocities of intermediate mass fragments produced in the mid-velocity region for peripheral collisions were found to show a particularly intriguing behavior. The shapes of the spectra were found to be invariant with respect to the incident energy. Some possible scenarios are discussed. For central collisions the onset and rapid rise of collective radial flow has been observed. The observed anisotropies in the flow pattern are studied within the SMM model.

## 1 INTRODUCTION

Both, central and peripheral collisions of symmetric heavy ions at intermediate energies, despite having been studied for decades now, are still drawing attention, still provide new pieces of information, and still contain open questions.

In order to study these reactions in more detail a series of experiments has been performed during the 4<sup>th</sup> INDRA Campaign carried out at the GSI. The reaction products formed using the beams delivered by the Heavy Ion Synchrotron SIS were measured with the  $4\pi$  mul-

tidetector system INDRA [1]. One of the systems studied at GSI was Au+Au at energies 40-150 A MeV. These reactions will constitute the main topic of this contribution.

Peripheral and mid-central collisions with their pronounced binary character allow to study the mechanism of dissipation: mass, charge, linear and angular momentum transfers leading to excitation of primary fragments. They are supposedly strongly influenced by dynamical processes. In these collisions, the 2 heaviest residua or their remnants remembering the entrance channel conditions, are usually accompanied by a sizable amount of par-

ticles and fragments with parallel velocities intermediate between those of the projectile and of the target [2-5] and their importance increases with increasing centrality of the collision. They are often referred to as *midrapidity* (*midvelocity*) emissions. The origin of these midrapidity fragments and related reaction scenarios are still debated and their characteristics are still a matter of interest. A few scenarios including fast pre-equilibrium particles, particles and fragments emitted from the neck, as well as light fission fragments preferentially aligned in between the two main reaction partners might be suggested here.

Investigation of the transverse velocities of fragments emitted at midrapidity in peripheral collisions led to the interesting observation of invariance of the velocity distributions with the incident energy. We will concentrate on this point in the first part of this contribution, after having introduced the chosen centrality selection.

Central collisions, in turn, provide a unique opportunity to study the multifragmentation phenomena and related physics of phase transition in finite pieces of nuclear matter as well as dynamical and collective effects such as flow, inseparably present on top of the thermal and Coulomb motion of the emitted fragments. The main assumption usually made here is that at some point in time during the reaction a thermal and chemical equilibrium is reached. With this assumption central collisions usually can be successfully described with the use of statistical models such as e.g. SMM[6]. The excess of kinetic energies of particles and fragments emitted in these reactions, and observed already around 35 A MeV [7, 8], is usually interpreted in terms of radial collective flow. The origin of this collective effect is still not well understood and several suggestions such as transparency or compression-decompression [9] might be put forward.

An interesting goal related to collective flow in the studied central Au+Au collisions is not only to quantify it, but also to study its angular distribution and anisotropy. This question

was extensively addressed by F. Lavaud and E. Plagnol (see [10]) and the main results of this investigation will be briefly presented in the second part of this contribution.

## 2 CENTRALITY SELECTION

Following previous investigations of symmetric heavy ion collisions [4, 5], we use in the following the total transverse energy,  $E_{\text{trans}12}$ , of LCP as an impact parameter selector.

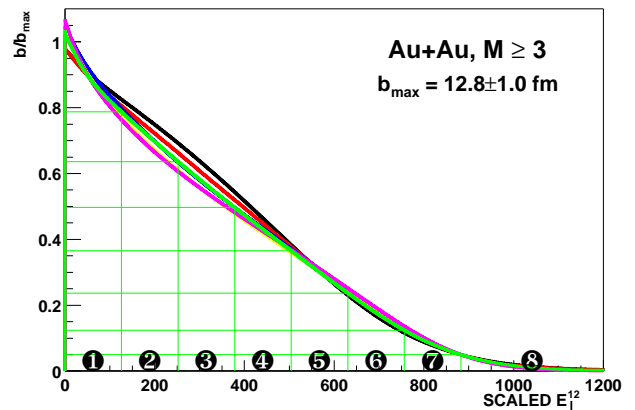


Figure 1: Reduced impact parameter derived from the transverse energy spectra of  $Z \leq 2$  particles from the Au+Au @ 40, 50, 60, 80, 100 and 150 A MeV. The spectra were scaled to the one for 40 A MeV. The indicated binning of  $E_{\text{trans}12}$  and  $b/b_{\text{max}}$  corresponds to Au+Au @ 60 A MeV reaction. Bin ① corresponds to the most peripheral collisions, bin ⑧ - to the most central ones.

Fig. 1 presents the relation between the scaled  $E_{\text{trans}12}$  and the reduced impact parameter,  $b/b_{\text{max}}$ , obtained with the use of the geometrical prescription [11]. The  $E_{\text{trans}12}$  spectra were scaled to the 40 A MeV one. The last bin (bin ⑧) corresponds to the most central 5% of the maximum impact parameter,  $b_{\text{max}}$ . The remaining part of the  $E_{\text{trans}12}$  spectrum was divided into 7 equal bins, with bin ① corresponding to the most peripheral collisions.

The total cross section for the Au+Au @ 40 A MeV reaction was estimated to be about 5.2 b for events with at least 3 charged particles detected. This corresponds to the maximum impact parameter of about 12.8 fm. The  $b_{\text{max}}$  is expected to increase with incident energy,

due to the Coulomb interaction, and should be about 6% larger at the highest energy (see e.g. [12]). This increase, however, is comparable with the accuracy of determining the  $b_{max}$ .

The observed scaling of Etrans12 in a broad incident energy range is worth stressing. The Etrans12 for the most central collisions (bin ③) scales linearly with the incident energy.

### 3 PERIPHERAL COLLISIONS: TRANSVERSE VELOCITY SCALING

Inspection of transverse velocities, or energies, for different rapidity bins leads to some interesting observations.

The upper row of Fig. 2 presents invariant cross sections for Li fragments from Au+Au @ 100 A MeV reaction, as a function of transverse velocity and rapidity with the indicated rapidity cuts. The middle row presents transverse velocity distributions of Li ions for different bombarding energies, and the bottom one the corresponding mean transverse energies.

At projectile rapidity and for peripheral collisions (left column) a Coulomb component in the velocity spectra is pronounced. The position of the peak is remarkably constant for all bombarding energies and indicates emission from the surface of the primary fragment.

The Coulomb component is nearly absent or possibly spread out over a wide velocity range in the emissions at midrapidity where one can observe two different scaling behaviors for the peripheral and central impact parameter bins. In the central case (right panel), the shapes are approximately Gaussian with an extra shoulder superimposed at lower incident energy, possibly due to Coulomb repulsion. Both, the mean and the width *increase* considerably with increasing bombarding energy and with the fragment mass (see also bottom right panel). This reflects the increasing importance of flow for central collisions at higher incident energies.

For peripheral reactions (middle column), a particularly intriguing behavior is observed.

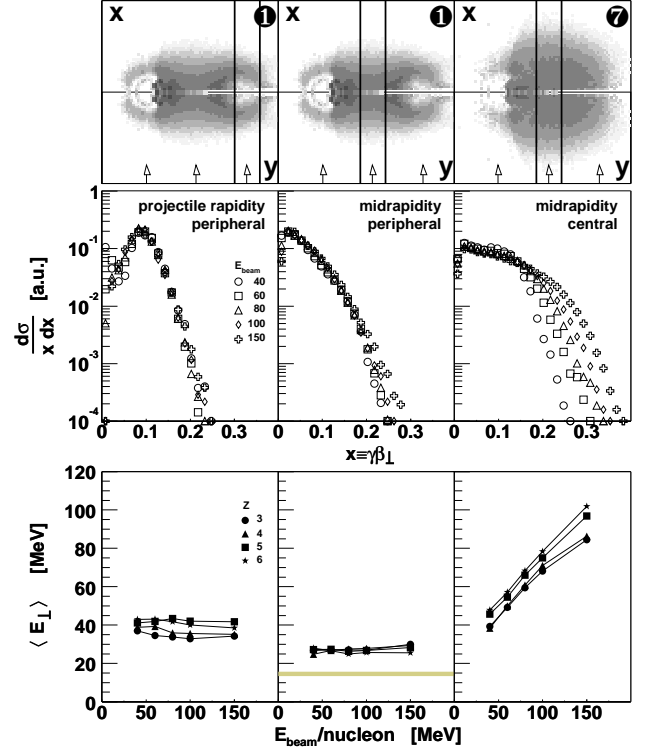


Figure 2: Top row: invariant cross sections for  $Z=3$  fragments as a function of transverse velocity ( $x$ ) and rapidity ( $y$ ) for Au+Au @ 100 A MeV reaction with the indicated rapidity cuts. The arrows denote, from the left, the target, CM, and projectile rapidities, respectively. Middle row: invariant transverse velocity distributions for  $Z=3$  at bombarding energies from 40 to 150 A MeV. Bottom row: mean transverse energies of IMFs with  $3 \leq Z \leq 6$  as a function of incident energy. The thick solid line represents the Goldhaber model prediction. The 3 columns correspond to 3 selections in rapidity and centrality: projectile rapidity and peripheral collisions (bin ①, left column), midrapidity and peripheral collisions (bin ②, middle column) and midrapidity and central collisions (bin ③, right column), respectively.

The shapes of the velocity spectra are between Gaussian and exponential and *invariant* with respect to the incident energy. The corresponding mean transverse energies of about 28 MeV for lithium ions seem too large for a purely thermal origin and are larger than the value of 14.6 MeV temperature obtained from the Goldhaber model [13] with  $p_F = 265$  MeV/c (the thick horizontal line) but may reflect the additional Coulomb potential that is generated by the two residua in the neck region.

Simulations of nucleon-nucleon collisions imply that the Pauli blocking of the collisions can

be partly responsible for this invariance. The mean transverse energies of nucleons scattered into the midrapidity region show a very weak dependence on incident energy provided Pauli blocking is effective. Otherwise, mean transverse energies increase with the incident energy. Within a coalescence picture one might expect invariance of mean transverse energies at midrapidity also for fragments.

#### 4 CENTRAL COLLISIONS: RADIAL FLOW AND DEFORMATION

As has already been demonstrated (Fig. 2, right column) central collisions are very sensitive to the incident energy. The analysis performed by F. Lavaud and E. Plagnol was done with a more elaborate impact parameter selection, using the concept of principal component analysis (PCA [14]), nevertheless, it was also demonstrated that the main conclusions hold true also for simple Etrans12 selection, when the 2 most central bins (7+8) are selected.

Fragment charge distributions are found to be fairly isotropic in the center of mass (CM) system for all energies studied (here: 40-100 A MeV). This observation supports the usage of a statistical approach to analyze the central collision data. Another interesting observation concerns the angular distribution of mean kinetic energies of fragments. These distributions show not only an excess of energy as compared to standard statistical model prediction, suggesting importance of collective effects, but also are found to be not at all isotropic in the CM system. They rather exhibit an enhancement along the beam axis (see symbols in Fig. 3). This, together with previous similar observations [15, 16], leads to the hypothesis of a non-spherical shape for the freeze-out volume. To quantify the amount of flow and its anisotropy in central collisions, the data were analyzed with the help of the SMM model. The best description of the data was achieved with the assumption of a prolate shape of the freeze-out volume and a self-similar, isotropic radial flow profile.

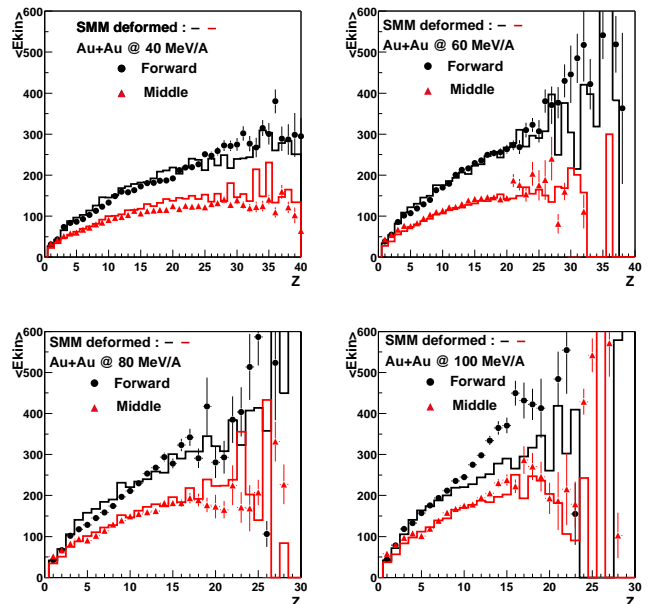


Figure 3: Comparison of the kinetic energy distributions for central Au+Au collisions as a function of a charge of the detected ion obtained at various incident energies for 2 angular regions (forward:  $0 \leq \theta_{cm} \leq 60$  degrees and middle:  $60 \leq \theta_{cm} \leq 120$  degrees). The histograms represent the SMM predictions with ellipsoidal freeze-out volume and self-similar radial flow.

The system at “freeze-out”, undergoing multifragmentation, can be characterized by its size:  $Z_o$ ,  $A_o$ , density  $\rho$  and thermal excitation energy  $E_o$ . Because of the pre-equilibrium effects the  $Z_o$ ,  $A_o$  and  $E_o$  at higher bombarding energies can differ substantially from the available charge, mass and kinetic energy. To find the freeze-out volume initial conditions an extensive search for parameters  $Z_o$ ,  $A_o$ ,  $E_o$  has been performed for a fixed  $\rho$  equal to 1/3 of the normal nuclear matter density ( $\rho_o$ ).

The fitting criterium was to reproduce with the filtered model results the experimental total charge of  $Z \geq 5$  fragments, their multiplicity, as well as the size of the heaviest fragment. The best fits were obtained for the parameters listed in the upper part of Tab. 1.

After having fixed the thermal properties of the contents of the freeze-out volume another search has been performed to extract the flow value and deformation. Now the goal of the fit was to reproduce the distribution of mean kinetic energies of fragments for different angu-

lar regions. The results of the fit can be viewed from the histograms in Fig. 3, and the fit parameters can be found in the bottom part of Tab. 1, where the “deformation” is defined as  $\sqrt{\langle E_{kin}(\theta_{CM} = 0) \rangle / \langle E_{kin}(\theta_{CM} = 90) \rangle}$ .

Table 1: Initial deformed freeze-out volume conditions together with the results of the fit to the mean kinetic energies of fragments.

$E_{beam}$ [A MeV]	40	60	80	100
$Z_o$	142	125	110	95
$A_o$	355	312	275	237
$E_o$ [A MeV]	6.0	7.8	8.7	9.1
deformation	2.1	2.0	1.7	1.5
radial flow [A MeV]	2.0	4.5	8.0	9.0
$E_{thermal}$ [%]	73	65	58	43

The presented procedure of extracting the flow characteristics and its results listed in Tab. 1 lead to some interesting conclusions.

First of all, the initial size of the system drops down from almost the whole system at 40 A MeV to close to half of it at 100 A MeV, indicating a strong increase of pre-equilibrium effects with increasing energy.

Secondly, although the available CM kinetic energy more than doubles (from 10 to 25 A MeV), the extracted thermal energies increase only by 50%. A large part of the remaining energy goes into radial flow, which evolves from 2 A MeV (1/3 of  $E_o$ ) to 9 A MeV (equal to  $E_o$ ). Altogether, the energy fraction converted into the thermalized source represents 73% at 40 A MeV and 43% at 100 A MeV (see bottom row of Tab. 1).

The origin of the deformation of the freeze-out volume is unclear. It could result from the way that the system reaches its maximum density point, a memory of the incoming direction could well be preserved during the following expansion. It could also originate from a partial transparency of the incoming ions. The fact that this deformation decreases with increasing beam energy could indicate that the nucleon-nucleon scattering becomes more important, because Pauli blocking is less effective, and hence the transparency less apparent.

## 5 SUMMARY

The presented contribution contained first results from the analysis of the experimental data on Au+Au reactions at energies from 40 to 150 A MeV, collected during the 4<sup>th</sup> INDRA campaign conducted at the GSI.

Transverse velocities at midrapidity for peripheral collisions were found to show a surprisingly weak dependence on incident energy. Simulations of nucleon–nucleon collisions imply that Pauli blocking of the collisions could be partly responsible for this invariance.

A detailed analysis of central collisions with the use of the SMM model showed that the best description of the data could be achieved with the assumption of a prolate shape of the freeze-out volume and a self-similar radial flow.

C. Sf. acknowledges the support of the Alexander von Humboldt Foundation.

## REFERENCES

- [1] J. Pouthas *et al.*, Nucl. Instr. Meth. in Phys. Res. **A357**, 418 (1995).
- [2] J.F. Dempsey *et al.*, Phys. Rev. C **54**, 1710 (1996).
- [3] Y. Larochele *et al.*, Phys. Rev. C **55**, 1869 (1997).
- [4] J. Lukasik *et al.*, Phys. Rev. C **55**, 1906 (1997).
- [5] E. Plagnol *et al.* Phys. Rev. C **61**, 014606 (2000).
- [6] J.P. Bondorf *et al.*, Phys. Rep. **257**, 133 (1995).
- [7] M. D’Agostino *et al.*, Phys. Lett. B371, 175(1996).
- [8] J.D. Frankland *et al.*, Nucl. Phys. A 689, 940 (2001).
- [9] C. Hartnack and J. Aichelin, Phys. Lett. B506, 261(2001).
- [10] F. Lavaud, PHD Thesis, Universite Louis Pasteur - Strasbourg I, 2001, (IPNO-T.01-06)
- [11] C. Cavata *et al.*, Phys. Rev. C **42**, 1760 (1990).
- [12] R. Bass, “Nuclear Reactions with Heavy Ions”, Springer-Verlag Berlin Heidelberg New York 1980.
- [13] A.S. Goldhaber, Phys. Lett. **53B**, 306 (1974).
- [14] P. Desesquelles, Ann. Phys. Fr. **20**, 1 (1995).
- [15] A. Le Fevre *et al.*, Phys. Rev. C 60, 051602 (1999).
- [16] B. Bouriquet *et al.*, Proc. XXXIX Intern. Wint. Meet. on Nucl. Phys., Bormio 2001, Italy, p. 84.